Constitutive modelling of fine-grained gassy soils

Zhiwei Gao[1*], Hongjian Cai[1], Yi Hong[2], Dechun Lu[3]

[1] James Watt School of Engineering, University of Glasgow, Glasgow, G12 8QQ, UK

[2] Key Laboratory of Offshore Geotechnics and Material of Zhejiang Province, College of Civil Engineering and Architecture, Zhejiang University, Hangzhou, 310058, China

[3] Key Laboratory of Urban Security and Disaster Engineering of Ministry of Education, Beijing University of Technology, Beijing 100124, China

[*] Corresponding author. Email: zhiwei.gao@glasgow.ac.uk; Tel: +44 1413303927

ABSTRACT: ine-grained marine sediments often contain gas bubbles that can cause many geotechnical problems. This soil has a composite structure with gas bubbles fitting within the saturated soil matrix. The gas cavity has a detrimental effect on the soil stiffness and strength when they are filled with undissolved gas only. The gas cavity can be filled with gas and pore water due to 'bubble flooding'. Bubble flooding has a beneficial effect on the soil stiffness and undrained shear strength because it makes the saturated soil matrix partially drained under a globally undrained condition. A critical state constitutive model for gassy clay is presented which accounts for the composite structure of the soil and bubble flooding. The gas cavity is assumed to have a detrimental effect on the plastic hardening of the saturated soil matrix. Some of the bubbles can be flooded by pore water from the saturated soil matrix which leads to higher mean effective stress of the saturated soil matrix. Consequently, both soil stiffness and strength increase. Only one new parameter is introduced to model the detrimental effect of gas bubbles on plastic hardening. The model has been validated by the results of three gassy clays.

Keywords: Gassy clay, critical state, constitutive model, undrained shear strength, pore pressure

1. INTRODUCTION

Submarine soils with free gas bubbles are widely seen in the seabed throughout the world (Hong et al., 2017; Gao et al., 2020; Sultan and Garziglia, 2014). Gas bubbles can also be encountered in onshore organic soils (Jommi et al., 2019). Most of the free gas is methane generated by soil decomposition and gas hydrate melting that will be affected by temperature and pressure (Sills et al., 1991; Sultan et al., 2012; Jommi et al., 2019). Since the soil decomposition and gas hydrate melting are faster at a higher temperature, more methane will be generated in the submarine soils as global warming continues (Milich, 1999; Stagg et al., 2017). Free gas has a dramatic influence on the mechanical behaviour of soils and is considered a major hazard for offshore ground engineering (Houlsby and Byrne, 2005; Sultan et al., 2012; Riboulot et al., 2013). Some failures of offshore foundations and large-scale submarine landslides have occurred due to the weakening effect of gas on the strength of seabed (Locat & Lee, 2002; Riboulot et al., 2013). A typical example includes the world's largest submarine slides (i.e., Storegga Slide), which is partly triggered due to the presence of gas within the marine sediments (Sultan et al., 2004). To assess and mitigate the geotechnical risks associated with gassy clay, it is important to have a proper understanding of the mechanical behaviour of this soil.

The mechanical behaviour of gassy clay is found to be affected by its unique internal structure with discrete gas cavities fitting within the saturated soil matrix. The gas phase in the soil is discontinuous while the water phase is continuous, which is different from conventional unsaturated soils close to the ground surface with a continuous gas phase. The gas bubbles make the soil more compressible due to their high compressibility. As the gas bubbles have no shear stiffness or shear strength, they tend to decrease the shear stiffness and strength of clay (Wheeler, 1986; Sultan et al., 2012; Riboulot et al., 2013). In some cases, however, pore water can drain into the gas cavities from the saturated soil matrix, making the saturated soil matrix partially drained in a globally undrained shearing test. This is called 'bubble flooding' by Wheeler (1986). Bubble flooding is shown to have a beneficial effect on

the undrained shear strength of gassy clay (Wheeler, 1988; Sham, 1989; Gao et al., 2020).

To describe the mechanical behaviour of gassy clay properly, it is crucial to consider the composite structure and bubble flooding. Nageswaran (1983) and Thomas (1987) have studied the compression behaviour of gassy clay. It is found that the soil volume change can be described by accounting for the gas compressibility. Bubble flooding does not occur in pure compression. Wheeler (1986) was the first to derive the lower and upper bounds for the undrained shear strength of gassy clay, where the composite soil structure and bubble flooding are accounted for. The lower bound was derived by assuming that the cavities have a detrimental effect on soil strength only. Bubble flooding is considered for the upper bound. This theory has been validated by test results on different gassy clays (Wheeler, 1986; Sham, 1989; Hong et al., 2017). But it cannot be used to predict the stress-strain behaviour and undrained shear strength for a specific loading condition.

Some attempts have been made in modelling the complete stress-strain relationship of gassy clay based on these early studies. Grozic et al. (2005) have proposed a constitutive model for this soil by considering the gas as part of the pore fluid, which cannot represent the real internal structure of this soil. Pietruszczak & Pande (1996) have developed a method for constitutive modelling of gassy soils based on the micromechanical analysis. Though it can consider the composite structure of gassy clay, it cannot capture the detrimental effect of gas bubbles on the undrained shear strength. Based on extensive laboratory studies, Hong et al. (2020) proposed a constitutive model for gassy clay by considering the effect of free gas on the dilatancy and yield surface shape. Gao et al. (2020) have developed a composite approach for constitutive modelling of gassy clay. Both these two recent models are capable of describing the detrimental and beneficial effect of free gas on the stiffness and strength of gassy clay. But the two models contain at least two extra parameters in addition to the classic critical state model for saturated clay (i.e., Modified Cam-clay model, or MCC model), some of which may not be easily obtained through conventional triaxial tests. Besides, the

gas pressure is employed as an internal variable in Gao et al. (2020), which causes incovinence for using the model: (i) it is almost impossible to measure the gas pressure in gassy clay either in the lab or the field; (ii) extra equations for estimating the initial gas pressure and evolution of gas pressure during loading are required; (iii) the elastic bulk modulus of water has to be used to derive the constitutive equations when the gas pressure is employed as a state variable (Gao et al., 2020).

A new critical state constitutive model for gassy clay is proposed in this study. It is based on the method proposed in Gao et al. (2020), which accounts for the composite internal structure and bubble flooding of gassy clay. The new model uses stress quantities which can be readily measured and only one parameter is introduced (as compared to the MCC model) to describe the effect of gas bubbles on the mechanical behaviour of clays, making it easy to calibrate and use. The soil response in triaxial compression and isotropic compression is considered in this study. Two stress quantities, the mean effective stress p $[(= \sigma_a + 2\sigma_r)/3]$ and deviator stress q $(= \sigma_a - \sigma_r)$ are used, where σ_a is the total axial stress and σ_r is the total radial stress. The volumetric strain ε_v $(= \varepsilon_a + 2\varepsilon_r)$ and shear strain ε_q $[= \frac{2}{3}(\varepsilon_a - \varepsilon_r)]$ are used in the constitutive equations, where ε_a is the axial strain and ε_r is the radial strain.

2. FRAMEWORK OF THE CONSTITUTIVE MODEL

This study focuses on the mechanical behaviour of normally consolidated clay with a fixed amount of free gas. Gas dissolution and exsolution due to the change in mean total stress is not considered (Sultan et al., 2012), as the two processes can be negligible for the gas types (mainly methane or nitrogen, which has very low solubility) of interests. The following assumptions are made for the new constitutive model based on existing research (Wheeler, 1988; Wheeler et al., 1990; Gao et al., 2020): (a) Gassy clay is a composite material with compressible cavities and saturated soil matrix (Fig. 1). The cavities are filled with gas when there is no bubble flooding. Once bubble flooding occurs, there are both gas and water in

the cavities (Wheeler, 1988; Gao et al., 2020). Bubble flooding makes the saturated soil matrix partially drained in a globally undrained test. Because there is water drainage from the soil but such water flow is insufficient to make the matrix fully drained. Terzaghi's effective stress principle works for the saturated soil matrix. The volume change of gassy clay is caused by both water flow at the soil element boundary and bubble flooding (Wheeler, 1988); (b) When there is no bubble flooding, the gas cavities have a detrimental effect on the soil strength only because gas bubbles have no shear stiffness and strength, causing stress concentration (and thus damage) around the cavities. Bubble flooding makes the mean effective stress of the saturated soil matrix increase, which has a beneficial effect on the stiffness and shear strength (Fig. 1b).

3. STRESS AND STRAIN VARIABLES FOR GASSY CLAY

As gassy clay is a composite, the rule of mixtures should be used to get the relationship between total stress and stress state of the saturated soil matrix (Pietruszczak & Pande, 1996; Gao and Diambra, 2020; Gao et al., 2020; Shi et al., 2019). Since the volume fraction of gas f is very small in most cases (less than 0.05), the following equations are used for stress dcomposition (Gao et al., 2020)

$$p_m = p \tag{1}$$

$$p'_m = p' = p - u_w \tag{2}$$

$$q_m = q \tag{3}$$

where p_m and p'_m are total and mean effective stress of the saturated clay matrix, q_m is the deviator stress of the saturated soil matrix, u_w is the pore water pressure. q is only dependent on q_m because the gas has no shear stiffness. Note that the assumption in Eqs. (1) and (2) is valid when the gas volume fraction is small and the gas pressure is close to the water pressure. As will be shown in the subsequent sections, the model can give reasonable prediction of gassy clay behaviour with this assumption. It could be due to that the gas pressure and water pressure are close, because the curvature of the air-water interface is small due to big gas bubble size (Wheeler, 1986). The volume fraction of cavities f is

expressed as below (Wheeler, 1988)

$$f = \frac{V_c}{V} \tag{4}$$

where V_c is the specific volume of cavities and V is the total specific soil volume. When there is no bubble flooding, the cavities are filled with free gas and one has

$$V_c = V_g = (1 - S_r)e \tag{5}$$

$$f = \frac{V_c}{V} = \frac{(1-S_r)e}{1+e} \tag{6}$$

where S_r ($= \frac{V_w}{V_v}$) is the degree of saturation and e is the global void ratio, with V_w and V_v being the specific volume of pore water and void, respectively. When there is bubble flooding, $V_c > V_g$ and Eq. (4) must be used to calculate f (Fig. 1). Following Gao et al. (2020), the global shear strain ε_q and volumetric strain of ε_v the gassy clay can be expressed as below

$$\varepsilon_q = \varepsilon_q^m \tag{7}$$

$$\varepsilon_v = (1 - f)\varepsilon_v^m + f\varepsilon_v^c \tag{8}$$

where the superscripts 'm' and 'c' represent the saturated soil matrix and gas cavities, respectively. Eq. (7) is assumed because the gas bubbles have no shear stiffness and the distortion of them follows that of the saturated matrix (Gao et al., 2020). But the term $f\varepsilon_v^c$ in Eq. (8) cannot be neglected due to bubble flooding and high compressibility of the gas bubbles (Gao et al., 2020). As gassy clay is considered as a composite, the constitutive equation for the soil needs to be obtained based on the constitutive model for saturated soil matrix and gas cavities, which will be presented in the subsequent sections.

4. CONSTITUTIVE RELATIONSHIP FOR THE SATURATED CLAY MATRIX

4.1 Volume change of the saturated soil matrix

The constitutive model for the saturated soil matrix is proposed based on the Modified Cam-Clay (MCC) model (Roscoe and Burland, 1968). The plastic hardening of the MCC is modified to incorporate the effect of gas cavities. Besides, the volumetric strain increment of the matrix $d\varepsilon_v^m$ is dependent on both water flow at the boundary dV_b and bubble flooding dV_f

which occurs inside the soil (Wheeler, 1986; Sills et al., 1991). The expression for $d\varepsilon_v^m$ is

$$d\varepsilon_v^m = \frac{dV_b}{V_m} + \frac{dV_f}{V_m} = d\varepsilon_v^b + d\varepsilon_v^f \quad (9)$$

where $d\varepsilon_v^b$ and $d\varepsilon_v^f$ denote the volumetric strain increments caused by water flow at the boundary and bubble flooding, respectively.

4.2 Constitutive equations for the saturated soil matrix

The yield function, plastic flow rule and elastic stress-strain relationship can be found in Gao et al. (2020). Since the pore gas pressure is not used in the current model, the plastic hardening law and bubble flooding equation are different, which will be discussed here. In a recent study (Gao et al., 2021), it is found that the variable $\frac{u_w+p_a}{p_c'}$ is suitable for modelling lower and upper bounds of the shear strength of gassy clay, where p_a is the atmospheric pressure and p_c' denotes the yield surface size. It will thus employed in the new model formulations.

The following hardening law is proposed for the saturated soil matrix

$$dp_c' = \langle L \rangle r_{pc} = \langle L \rangle (r_1 - r_2) = \langle L \rangle \frac{(1+e_0)p_c'}{\lambda-\kappa}\frac{\partial F}{\partial p'}\left[1 - a\sqrt{f}\,\frac{\eta}{\mathrm{M}}\left(1 - \mathrm{e}^{-\frac{u_w+p_a}{p_c'}}\right)\right] \quad (10)$$

where p_c' denotes the size of MCC yield surface, L is the loading index, e_0 is the initial value of the saturated matrix void ratio e_m, $\eta\ (= q/p')$ is the stress ratio, λ is the compression index, κ is the swelling index, F is the MCC yield function, p_a is the atmospheric pressure, $\langle\ \ \rangle$ are the McCauley brackets [$\langle L \rangle = L$ for $L > 0$ and $\langle L \rangle = 0$ otherwise] and a is a new model parameter. r_1 is the same as that for the MCC model and the the term r_2 is used to model the detrimental effect of gas bubbles on the plastic hardening and shear strength. Higher r_2 indicates more detrimental effect of gas bubbles on plastic hardening and shear strength. $r_2 = 0$ when there is no cavity with $f = 0$. Existing experimental evidence shows that the gas bubbles merely influence the plastic hardening of saturated soil matrix in isotropic consolidation, and therefore, the term $\frac{\eta}{\mathrm{M}}$ is introduced to make $r_2 = 0$ at $\eta = 0$ (Thomas, 1987; Wheeler, 1986; Hong et al., 2020). When the gassy soil is subjected to shear

(e.g., triaxial compression), the detrimental effect of gas bubbles on plastic hardening is higher as $\frac{u_w+p_a}{p_c'}$ increases, but such detrimental effect is limited (Wheeler, 1988; Hong et al., 2020; Gao et al., 2021). Therefore, the term $1-\mathrm{e}^{-\frac{u_w+p_a}{p_c'}}$ is used to make r_2 increase with $\frac{u_w+p_a}{p_c'}$ and reach the maximum value of 1 when $\frac{u_w+p_a}{p_c'}$ is big enough. The plastic modulus K_p for the saturated matrix is

$$K_p = -\frac{\partial F}{\partial p_c'} r_{pc} \tag{11}$$

4.3 Bubble flooding

The concept of bubble flooding was first proposed by Wheeler (1986) to explain the beneficial effect of gas bubbles on undrained shear strength of gassy clay. For each bubble, the condition of bubble flooding is $u_g \approx u_w$, where u_g is the gas pressure (Wheeler, 1986). Since $u_g > u_w$ due to the surface tension of water meniscus, $u_g \approx u_w$ is more likely when u_w increases, which makes the curvature of water meniscus reduce and the difference between u_g and u_w smaller. Therefore, it is assumed that bubble flooding occurs when u_w increases. The following formulation is proposed for $d\varepsilon_v^f$

$$d\varepsilon_v^f = A du_w \tag{12}$$

where

$$A = \begin{cases} \frac{(1-s_r)e}{(u_w+p_a)(1+e)} & \text{for } du_w > 0 \\ 0 & \text{for } du_w \le 0 \end{cases} \tag{13}$$

It is evident that there is bubble flooding only when the soil is unsaturated with $s_r < 1$ and $du_w > 0$ (Gao et al., 2020). The rate of bubble flooding is also higher when u_w is smaller, which is supported by the experimental observation that gas cavities have a less beneficial effect on the strength of clay when u_w is higher (Wheeler, 1986; Sham, 1989; Hong et al., 2020). In drained isotropic compression, bubble flooding will not occur based on Eq. (12) because u_w is constant. As will be shown in the subsequent sections of this paper, this assumption is reasonable for modelling the volume change of gassy clay in drained isotropic

compression (Figs. 5 and 9). However, if we devise an isotropic compression test with partial drainage (e.g., u_w increases), the model will predict some bubble flooding. Note that Eq. (12) can predict bubble flooding even when there is a small variation in u_w, which is not realistic because this may not bring u_w close to u_g. This limitation will be addressed in future research.

5. GAS AND CAVITY VOLUME CHANGE

Since the cavity surface is part of the saturated soil matrix, it is expected that the cavity changes size when the effective stress of saturated soil matrix changes (or there is deformation in the matrix). Therefore, the volumetric strain increment of the cavity $d\varepsilon_v^c$ is assumed to be affected by dp'

$$d\varepsilon_v^c = \frac{dV_c}{V_c} = Bdp' = \frac{1}{p'+u_w+p_a}dp' \tag{14}$$

where dV_c is the volume change of the cavity. This equation indicates that the compressibility of the cavity is dependent on the stiffness of saturated soil matrix as p' is included. Higher p' will lead to lower compressibility of both the saturated soil matrix and gas cavity. In addition, the cavity volume change may also depend on other soil properties like the plasticity index and particle size, which means that extra model parameters may be required to describe such influence. But it is found that Eq. (14) is suitable for modelling the gas volume change (see Figs. 5 and 9 below). Therefore, it is unnecessary to use more complex formulations for the gas volume change.

6. THE CONSTITUTIVE EQUATION AND PARAMETER DETERMINATION

The constitutive equation for the entire gassy soil can be derived based on the constitutive model for the saturated soil matrix and equations for cavity and gas volume evolution, which is presented in this section. In the present model, the total strain increment is assumed to be the summation of the elastic and plastic parts with $d\varepsilon_v^m = d\varepsilon_v^{me} + d\varepsilon_v^{mp}$ and $d\varepsilon_q^m = d\varepsilon_q^{me} + d\varepsilon_q^{mp}$. Based on Eqs. (8) and (14), one can get the following

$$d\varepsilon_v = (1-f)d\varepsilon_v^m + fBdp' \tag{15}$$

Since $d\varepsilon_v^m = d\varepsilon_v^{me} + d\varepsilon_v^{mp} = \frac{dp'}{K_m} + \langle L\rangle \frac{\partial F}{\partial p'}$, Eq. (15) can be rewritten as

$$d\varepsilon_v = (1-f)\left(\frac{dp'}{K_m} + \langle L\rangle \frac{\partial F}{\partial p'}\right) + fBdp' \tag{16}$$

The expression of dp' can be obtained based on Eq. (16) as below

$$dp' = \frac{d\varepsilon_v - (1-f)\langle L\rangle \frac{\partial F}{\partial p'}}{\frac{1-f}{K_m} + fB} = \frac{d\varepsilon_v}{X} - \langle L\rangle \frac{1-f}{X}\frac{\partial F}{\partial p'} \tag{17}$$

where X represents the denominator of Eq. (17). Combining Eq. (17) and the condition of consistency for the yield function of MCC, one has

$$\frac{\partial F}{\partial p'}\left[\frac{d\varepsilon_v}{X} - \langle L\rangle \frac{1-f}{X}\frac{\partial F}{\partial p'}\right] + 3G_m \frac{\partial F}{\partial q}\left[d\varepsilon_q - \langle L\rangle \frac{\partial F}{\partial q}\right] - \langle L\rangle K_p = 0 \tag{18}$$

The loading index L can then be determined using Eq. (18)

$$L = \frac{\frac{1}{X}\frac{\partial F}{\partial p'}d\varepsilon_v + 3G_m \frac{\partial F}{\partial q}d\varepsilon_q}{K_p + \frac{1-f}{X}\left(\frac{\partial F}{\partial p'}\right)^2 + 3G_m\left(\frac{\partial F}{\partial q}\right)^2} = \Lambda_p d\varepsilon_v + \Lambda_q d\varepsilon_q \tag{19}$$

where Λ_p and Λ_q are self-evident. The expression of dp' in terms of $d\varepsilon_v$ and $d\varepsilon_q$ can be obtained using Eqs. (17) and (19)

$$dp' = C_{pp}d\varepsilon_v + C_{pq}d\varepsilon_q \tag{20}$$

where

$$C_{pp} = \frac{1}{X} - h(L)\Lambda_p \frac{1-f}{X}\frac{\partial F}{\partial p'} \tag{21}$$

$$C_{pq} = -h(L)\Lambda_q \frac{1-f}{X}\frac{\partial F}{\partial p'} \tag{22}$$

where $h(L)$ is the Heaviside function with $h(L) = 1$ when $L > 0$ and $h(L) = 0$ otherwise. The increment of the deviator stress dq is

$$dq = 3G_m\left(d\varepsilon_q - d\varepsilon_q^{mp}\right) = 3G_m\left(d\varepsilon_q - \langle L\rangle \frac{\partial F}{\partial q}\right) = C_{qp}d\varepsilon_v + C_{qq}d\varepsilon_q \tag{23}$$

where

$$C_{qp} = -h(L)3G_m\Lambda_p \frac{\partial F}{\partial q} \tag{24}$$

$$C_{qq} = 3G_m - h(L)3G_m\Lambda_q \frac{\partial F}{\partial q} \tag{25}$$

Combining Eqs. (8), (12), (14) and (20), the following equation can be got

$$d\varepsilon_v = (1-f)(d\varepsilon_v^b + A du_w) + fB\left(C_{pp} d\varepsilon_v + C_{pq} d\varepsilon_q\right) \quad (26)$$

Eq. (26) can then be used to get the expression for du_w

$$du_w = C_{wp} d\varepsilon_v + C_{wq} d\varepsilon_q + C_{wb} d\varepsilon_v^b \quad (27)$$

where

$$C_{wp} = \frac{1 - fBC_{pp}}{(1-f)A} \quad (28)$$

$$C_{wq} = -\frac{fBC_{pq}}{(1-f)A} \quad (29)$$

$$C_{wb} = -\frac{1}{A} \quad (30)$$

The constitutive equation can be written in a matrix form as below

$$\begin{bmatrix} dp' \\ dq \\ du_w \end{bmatrix} = \begin{bmatrix} C_{pp} & C_{pq} & 0 \\ C_{qp} & C_{qq} & 0 \\ C_{wp} & C_{wq} & C_{wb} \end{bmatrix} \begin{bmatrix} d\varepsilon_v \\ d\varepsilon_q \\ d\varepsilon_v^b \end{bmatrix} \quad (31)$$

The constitutive equation requires two volumetric strain quantities ε_v and ε_v^b, which represent the total volume change and volume change due to water flow at the boundary. This is due to the bubble flooding and cavity volume change in the soil, which makes ε_v and ε_v^b different. Implementation of the model has been discussed in Gao et al. (2020).

There are six parameters in the model, five of which are the same as those for the MCC model. Only the parameter a in Eq. (10) should be determined for gassy clay. Since a is used to describe the detrimental effect of gas bubbles on plastic hardening and shear strength, it must be determined using the triaxial compression test data on gassy clay. Only one set of test data from the conventional triaxial compression test is needed for determining a through best fitting the stress-strain relationship. A test with an initial degree of saturation $S_{r0} \leq 0.95$ where the effect of gas on the soil response is obvious is recommended. Determination of a will be presented below using the test data of gassy Combwich mud (Wheeler, 1986).

7. MODEL VALIDATION

The model will be validated against the test data on three gassy clays, including Gassy

Combwich mud (Wheeler, 1986), Gassy Kaolin (Sham, 1989) and Gassy Malaysian Kaolin (Hong et al., 2020).

7.1 Gassy Combwich mud (Wheeler, 1986)

Both isotropic consolidation and undrained triaxial compression tests have been reported on gassy Combwich mud in Wheeler (1986). The parameters M, λ and N are directly obtained from Wheeler (1986). The elastic parameter $\nu = 0.2$ is assumed as it has a small influence on the model prediction. Finally, a is determined using the undrained test data on gassy Combwich mud with initial mean effective stress $p'_0 = 400$ kPa, initial pore water pressure $u_{w0} = 0$ and initial degree of saturation $S_{r0} = 0.95$ (Fig. 2). The undrained shear strength is higher when a is smaller, which describes a less detrimental effect of gas bubbles on the soil stiffness and strength (Fig. 2). The best model prediction for the undrained shear strength and effective stress path can be obtained by using $a = 14$. All the model parameters are listed in Table 1.

The undrained shear strength of the gassy clay shown in Fig. 2 is higher than that of the saturated soil. This is because of the beneficial effect caused by bubble flooding dominates for the gassy soil, which is illustrated in Fig. 3. The model prediction without bubble flooding is shown in Fig. 3 ($A = 0$ in Eq. 13). All the model parameters are the same as those in Table 1. The undrained shear strength predicted by neglecting bubble flooding is smaller than the saturated one, as bubbles are assumed to have a detrimental effect on the soil stiffness and strength only with $a = 14$. Under other conditions of u_{w0}, S_{r0} and p'_0, the overall effect of gas bubbles on undrained shear strength can become detrimental due to a smaller amount of bubble flooding, which has been discussed in the second assumption for the model.

Though many undrained triaxial compression tests have been done by Wheeler (1986), only one complete set of data is available, which includes the effective stress path and shear stress-strain relationship (see Fig. 2). For the other tests, only the undrained shear strength

s_u is available, which will be used to validate the model prediction. Fig. 4 shows the model prediction for the undrained shear strength of gassy Combwich mud with different p_0' and u_{w0}. The model prediction captures the trends of s_u variation with S_{r0} well, including both beneficial and detrimental effects under different circumstances. Obvious overestimation is observed for the tests with $p_0' = 200$ kPa and $u_{w0} = 100$ kPa (Fig. 4b). There are two possible reasons for this discrepancy. First, the s_u for the test with $p_0' = 400$ kPa, $u_{w0} = 0$ kPa and $u_{w0} = 0.95$, which has been used for determining the parameter a, lies on the upper bound of the test data in its group (Fig. 4a). This indicates that the model prediction tends to give higher s_u for most of the tests. A better model prediction is expected if more results like those in Fig. 2 are available for getting more optimum value of a. Besides, it is noticed that the data for this group of tests are quite scattered, with two tests ($S_{r0} = 0.97$ and $S_{r0} = 0.984$) showing unexpectedly low s_u (Fig. 4b). The real s_u could be higher and closer to the model prediction.

Fig. 5 presents the comparison between test data and model prediction of gassy Combwich mud in isotropic compression (Wheeler, 1986). The dots and lines represent the test data and model predictions, respectively. The initial degree of saturation S_{r0} is the one at $p' = 100$ kPa. For the gassy soil samples, the total volume change is caused by water drainage from the saturated soil matrix and compression of gas bubbles (Eq. 14). There is no bubble flooding as u_w is a constant (Eq. 12). The model can satisfactorily describe the volume change of gassy clay with different S_{r0} (Fig. 5a), indicating that Eq. (14) is suitable for modelling gas cavity compression in gassy clay. There is a unique relationship between the matrix void ratio e_m and p' for all samples (Fig. 5b), because Terzaghi's effective stress principle works in the saturated soil matrix.

7.2 Gassy Kaolin (Sham, 1989)

A series of undrained triaxial compression tests have been carried out on Kaolin with helium to investigate the upper and lower bounds for the undrained shear strength of gassy clay (Sham, 1989). Details of the test procedure can be found in Sham (1989). The MCC parameters are determined using the same method as for Combwich mud. The parameter a is determined using the test data shown in Fig. 6, which is the only set of data which includes the stress-strain relationship and effective stress path. The model is then used to predict the s_u of all the other gassy Kaolin specimens under different combinations of p_0' and u_{w0} (Fig. 7). The predicted s_u is close to the measured value for most cases except those with $p_0' = 100$ kPa and $u_{w0} = 300$ kPa (Fig. 7d). Close inspection shows that the initial value of $\frac{u_w+p_a}{p_c'}$ is the maximum for this group of tests. This means that Eq. (10) tends to underestimate the detrimental effect of gas bubbles on the shear strength of this soil at higher $\frac{u_w+p_a}{p_c'}$. An improved model prediction can be achieved by introducing more model parameters, which will inevitably make the parameter determination more difficult.

7.3 Gassy Malaysian kaolin (Hong et al., 2020)

A group of undrained triaxial tests have been carried out on gassy Malaysian kaolin (MK) to validate the model. The liquid limit and plastic limit of MK is 65% and 28%, respectively (Hong et al., 2017). According to the plasticity chart (BSI 1999), this soil can be categorized as high plastic silt. The gas used in the tests is nitrogen. To get gassy soil samples with uniform and repeatable distribution of gas bubbles, the zeolite molecular sieve technique has been used (Nageswaran 1983; Wheeler 1988; Sills et al. 1991; Hong et al., 2020). A more detailed discussion of the sample preparation method can be found in Hong et al. (2017; 2020). The tests have been carried out using the GDS triaxial apparatus with a double-cell (i.e., HKUST cell (Ng et al., 2002)) and a differential pressure transducer (DPT). Before triaxial compression, each specimen was isotropically consolidated to an initial effective mean effective stress of $p_0' = 200$ kPa with different u_{w0}.

All the MCC parameters are determined using the test results in Figs. 8 and 9 on the saturated soil. In Fig. 8, the dots and lines denote the test results and model predictions, respectively. In isotropic consolidation with constant pore water pressure, there is no bubble flooding and the gas bubbles do not affect plastic hardening (Eq. 10). But there is extra gas bubble compression for unsaturated soil samples in isotropic consolidation (Eq. 14), which makes the slope of their $e - p'$ curves higher than that of the saturated soil (Fig. 9). The model gives a unique $e_m - p'$ relationship, which is identical to the $e - p'$ curve for the saturated soil. The parameter a is determined using the results on gassy clay in undrained triaxial compression tests with $p'_0 = 200$ kPa and initial pore water pressure $u_{w0} = 150$ kPa (Fig. 10). The model predictions for the other undrained triaxial compression tests are shown in Figs. 11 and 12. In general, the model has reproduced both detrimental and beneficial effect of gas on the soil response with various combinations of u_{w0} and S_{r0}.

It is noticed that gassy Malaysian kaolin silt has a much smaller a than gassy Combwich mud and Kaolin (Table 1). This indicates that the gas bubbles have a much smaller detrimental effect on the s_u of Malaysian kaolin. Hong et al. (2020) have shown that this is maybe linked with the difference in the plastic index (PI) of the soil. The more detrimental effect of gas on the soil strength is observed when the PI is higher. Among the three clays, the Malaysian kaolin has the lowest PI while the Kaolin in Sham (1989) has the highest. Indeed, the parameter a is the biggest for the Kaolin and smallest for the Malaysian kaolin silt (Table 1). Therefore, the parameter could be alternatively approximated based on the PI of each soil. But the undrained triaxial tests on Malaysian kaolin silt have been performed with the same p'_0. More tests on Malaysian kaolin with different p'_0 need to be done to confirm the correlation between PI and a.

CONCLUSION

A critical state constitutive model for gassy clay is proposed, in which the soil is considered as a composite material with saturated soil matrix and cavities. The cavities tend to have a

damaging effect on the soil structure as the gas has high compressibility and zero shear strength. In some cases, the cavities can be flooded by pore water, which makes the saturated soil matrix partially drained in an undrained test. Bubble flooding has a beneficial effect on soil stiffness and strength. The new model has the following features:

(a) Plastic hardening of the saturated soil matrix is assumed to be affected by gas cavities to model the damaging effect of gas cavities on the soil structure. As the gas volume fraction increases, the shear stiffness and strength of the soil decreases;

(b) The beneficial effect of free gas on soil strength and stiffness is modelled by considering bubble flooding. Bubble flooding is assumed to occur in all gassy soils in shear. But the amount of bubble flooding is dependent on the stress state and pore water pressure change.

(c) There are six parameters in the model, five of which are the same as those for the MCC model. Only one extra parameter is introduced to describe the damaging effect of gas bubbles on plastic hardening of the saturated soil matrix. It can be readily determined using the triaxial compression test data. The model has been validated by the results of over 100 tests on three gassy clays.

Future work will be done in the two aspects: (a) The formulation for describing the plastic hardening, bubble flooding and cavity volume change need to be futher improved to capture gassy clay behaviour with different properties. More extensive laboratory tests on this soil is needed for this work; (b) The model will be implemented in an open-source software package to solve real boundary value problems associated with gassy clay, enabling the assessment of geo-hazards such as submarine landslides of the gassy seabed. The main code will be modified to account for bubble flooding; (c) When a gassy soil sample is subjected to unloading, there can be gas exsolution that damages the soil structure (Sultan et al., 2012). The current model cannot capture the behaviour of gassy clay under unloading because it gives a purely elastic response. More research will be done to extend the model for such loading conditions.

ACKNOWLEDGEMENT

The third author gratefully acknowledges the financial support provided by the National Natural Science Foundation of China (41769523). The fourth author would like to acknowledge the financial support of The National Science Fund for Distinguished Young Scholars of China (51779221).

LIST OF SYMBOLS

e	Global void ratio
e_0	Initial void ratio
F	Yield function
f	Volume fraction of gas cavities
G_m	Elastic shear modulus of the saturated soil matrix
K_m	Elastic bulk modulus of the saturated soil matrix
K_p	Plastic modulus for the saturated soil matrix
L	Loading index
p	Total stress
p_c'	Initial mean effective stress
p_m	Total effective stress of the saturated clay matrix
p_m'	Mean effective stress of the saturated clay matrix
p_a	Atmospheric pressure
q	Deviator stress
q_m	Deviator stress of the saturated clay matrix
S_r	Degree of saturation
S_{r0}	Initial degree of saturation
s_u	Undrained shear strength
u_w	Pore water pressure
u_{w0}	Initial pore water pressure

V	Total specific soil volume
V_c	Specific volume of the cavity
V_w	Specific volume of pore water
V_v	Specific volume of void
V_m	Specific volume of the saturated soil matrix
V_g	Specific volume of gas bubbles
V_f	Specific volume of bubble flooding
ε_a	Axial strain
ε_r	Radial strain
ε_q	Shear strain
ε_v	Volumetric strain
ε_v^c	Volumetric strain of gas cavities
ε_v^m	Volumetric strain of saturated soil matrix
ε_v^b	Volumetric strain of water flow at the boundary
ε_v^f	Volumetric strain due to bubble flooding
ε_q^m	Shear strain of saturated soil matrix
ε_v^{me}	Elastic volumetric strain of saturated soil matrix
ε_v^{mp}	Plastic volumetric strain of saturated soil matrix
ε_q^{me}	Elastic shearc strain of saturated soil matrix
ε_q^{mp}	Plastic shear strain of saturated soil matrix
M	Critical state stress ratio
σ_a	Total axial strain
σ_r	Total radial strain

REFERENCES

Gao Z, Diambra A. (2020). A multiaxial constitutive model for fibre-reinforced sand. Géotechnique.1-13.DOI: 10.1680/jgeot.19.p.250.

Gao Z, Hong Y, Wang L. (2020). Constitutive modelling of fine-grained gassy soil: A composite approach. Numerical and Analytical Methods in Geomechnics (Accepted for publication). DOI: 10.1002/nag.3065.

Gao, Z. and Cai, H. (2021) Effect of total stress path and gas volume change on undrained shear strength of gassy clay. International Journal of Geomechanics (Accepted for Publication)

Grozic JLH, Nadim F, Kvalstad TJ. (2005). On the undrained shear strength of fine-grained gassy soils. Computers and Geotechnics. 32(7): 483–490. DOI: 10.1016/j. compgeo.2005.10.002.

Hong Y, Wang LZ, Ng CW, Yang B. (2017). Effect of initial pore pressure on undrained shear behaviour of fine-grained gassy soil. Canadian Geotechnical Journal. 2017; 54(11): 1592–1600. DOI: 10.1139/cgj-2017-0015.

Hong Y, Wang LZ, Zhang JF, Gao ZW. (2020). 3D elastoplastic model for fine-grained gassy soil considering the gas-dependent yield surface shape and stress-dilatancy. Journal of Engineering Mechanics. 146(5): 04020037. DOI: 10.1061/ (asce)em.1943-7889.0001760.

Houslby GT, Byrne BW. (2005). Design procedures for installation of suction caissons in clay and other materials. Proceeding of the Institution of Civil Engineers-Geotechnical Engineering. 2005;158(2): 75-82. DOI:10.1680/geng.2005.158.2. 75.

Jommi C, Muraro S, Trivellato E, Zwaneburg C. (2019). Experimental results on the influence of gas on the mechanical response of peats. Géotechnique. 69(9):753-766. DOI: 10.1680/jgeot.17.p.148.

445 Locat J, Lee HJ. (2002). Submarine landslides: advances and challenges. Canadian
446 Geotechnical Journal. 39(1): 193–212.DOI: 10.1139/t01-089.

447 Milich L. (1999). The role of methane in global warming: where might mitigation strategies
448 be focused? Global Environmental Change. 9(3): 179–201.DOI: 10.1016/s0959-
449 3780(98)00037-5.

450 Nageswaran S. (1983). Effect of gas bubbles on the sea-bed behaviour. PhD thesis, 1983;
451 Oxford University.

452 Ng, C. W., Zhan, L. T., & Cui, Y. J. (2002). A new simple system for measuring volume changes
453 in unsaturated soils. Canadian geotechnical journal, 39(3), 757-764.

454 Pietruszczak S, Pande GN. (1996). Constitutive relationships for partially saturated soils
455 containing gas inclusions. Journal of Engineering Mechanics. 122(1) 50–59. DOI:
456 10.1061/(asce)0733-9410(1996)122:1(50).

457 Roscoe KH, Burland JB. (1968). On the generalized stress-strain behaviour of 'wet' clay.
458 Engineering plasticity (eds. J. Heyman and F. A. Leckie), Cambridge University Press,
459 Cambridge, UK, 535–609.

460 Sham WK. (1989). The undrained shear strength of soils containing large gas bubbles. PhD
461 thesis. The Queen's University of Belfast.

462 Shi XS, Zhao J, Yin J, Yu, Z. (2019). An elastoplastic model for gap-graded soils based on
463 homogenization theory. International Journal of Solids and Structures. 163: 1-14.DOI:
464 10.1016/j.ijsolstr.2018.12.017.

465 Sultan N, Cochonat P, Foucher J P, et al. Effect of gas hydrates melting on seafloor slope
466 instability. Marine Geology, 2004, 213(1): 379-401.

467 Riboulot V, Cattaneo A, Sultan N, Garziglia S, Ker S, Imbert P, Voisset M. (2013). Sea-level
468 change and free gas occurrence influencing a submarine landslide and pockmark

formation and distribution in deepwater Nigeria. Earth and Planetary Science Letters. 375:78-91. DOI: 10.1016/j.epsl.2013.05.013.

Sills GC, Wheeler SJ, Thomas SD, Gardner TN. (1991). Behaviour of offshore soils containing gas bubbles. Géotechnique. 41(2): 227–241. DOI: 10.1680/geot. 1991.41.2.227.

Sultan, N., & Garziglia, S. (2014). Mechanical behaviour of gas-charged fine sediments: model formulation and calibration. Géotechnique. 64(11), 851-864.

Stagg CL, Schoolmaster DR, Krauss KW, Cormier N, Conner WH. (2017). Causal mechanisms of soil organic matter decomposition: deconstructing salinity and flooding impacts in coastal wetlands. Ecology. 98(8): 2003-2018. DOI: 10.1002/ ecy.1890.

Sultan N, De Gennaro V, Puech A. (2012). Mechanical behavior of gas-charged marine plastic sediments. Géotechnique. 62(9): 751–766. DOI: 10.1680/geot.12.og.002.

Thomas SD. (1987). The consolidation behaviour of gassy soil. PhD thesis, 1987; Oxford University.

Tsai SW, Hahn HT. (1980). Introduction to Composite Materials. Technomic.

Wheeler SJ. (1986). The stress-strain behaviour of soils containing gas bubbles. PhD thesis, Oxford University.

Wheeler SJ. (1988). A conceptual model for soils containing large gas bubbles. Géotechnique. 38(3): 389–397. DOI: 10.1680/geot.1988.38.3.389.

Wheeler SJ, Sham WK, Thomas SD. (1990). Gas pressure in unsaturated offshore soils. Canadian Geotechnical Journal. 27(1): 79–89. DOI: 10.1139/t90-008.

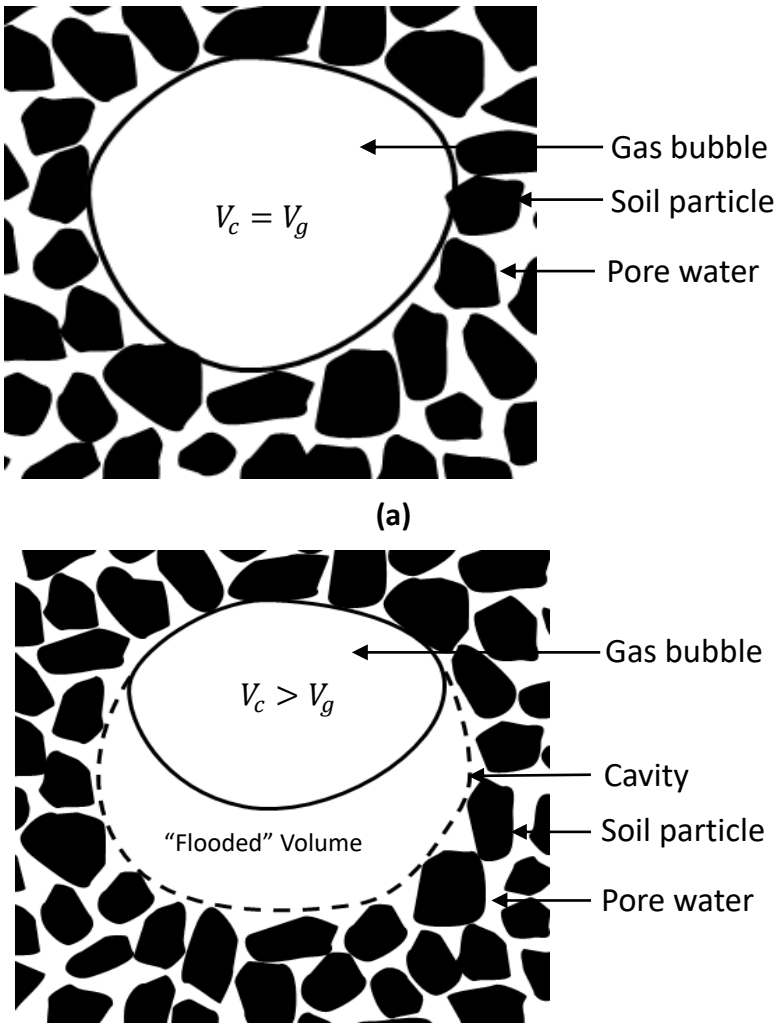

Fig. 1 Gas cavities filled by (a) free gas and (b) free gas and pore water

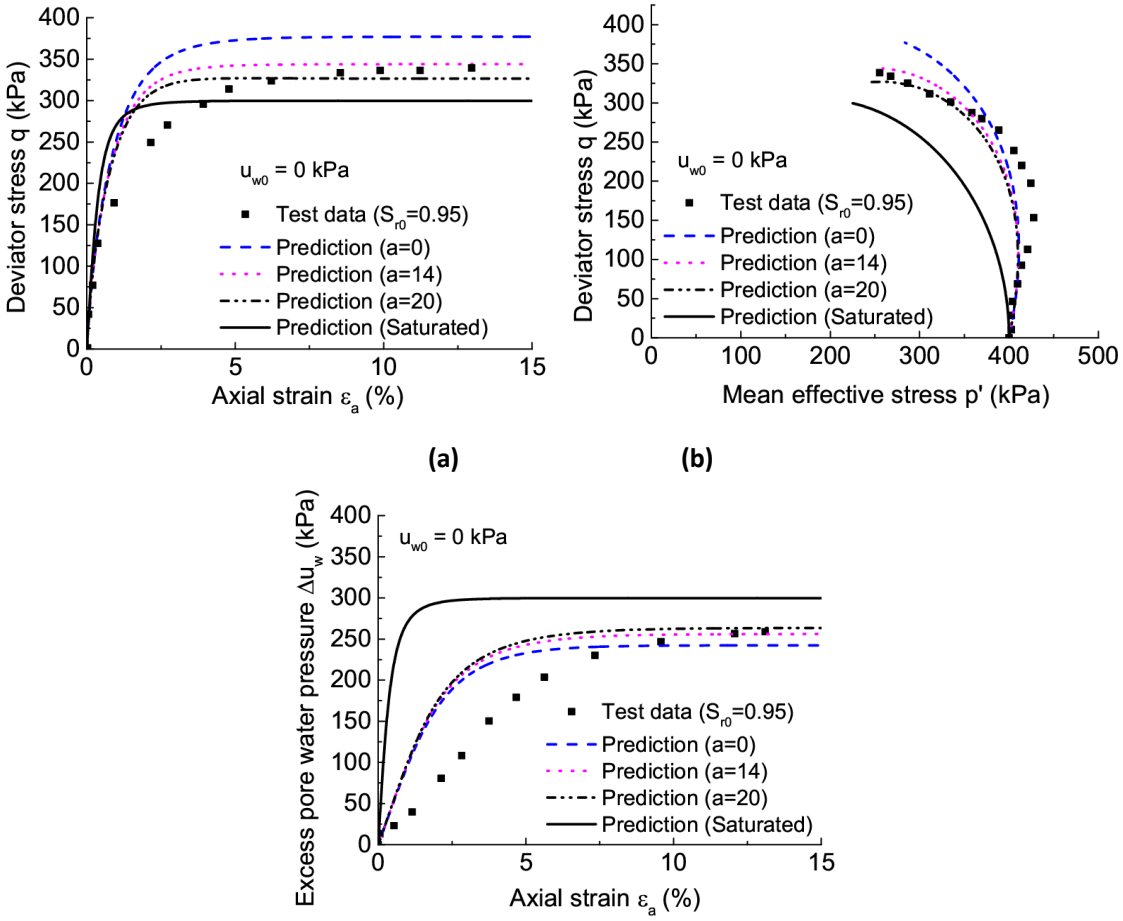

Fig. 2 Model prediction for shear behaviour of gassy Combwich mud: (a) the $\varepsilon_a - q$ relationship; (b) the effective stress path and (c) the evolution of excess pore water pressure

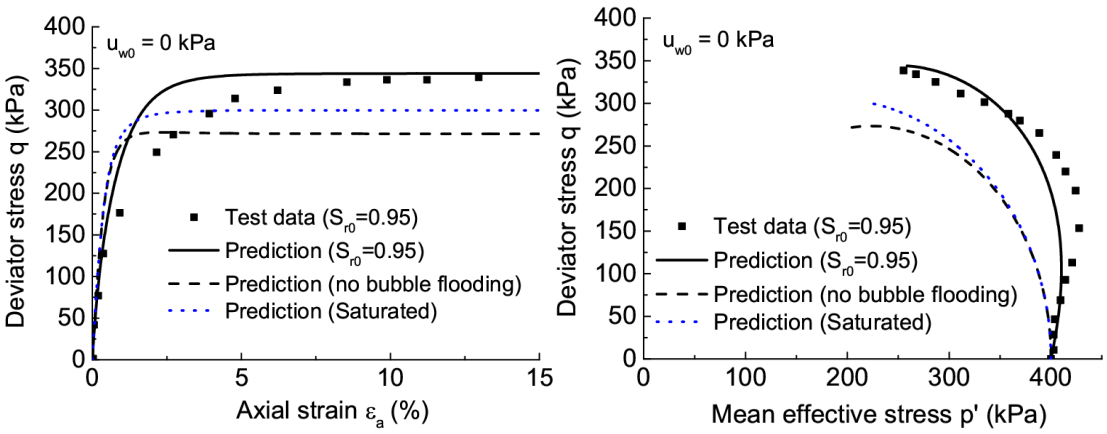

512

513 **(a)** **(b)**

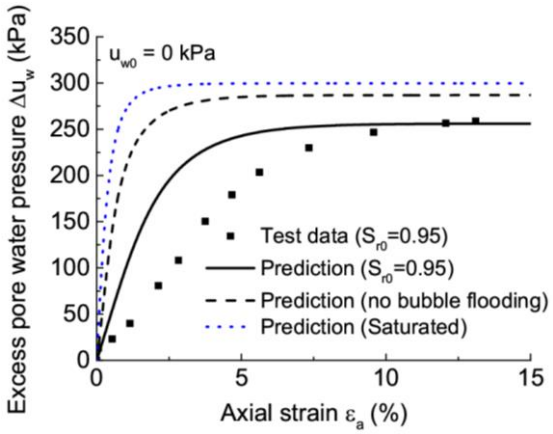

514

515 **(c)**

516 **Fig. 3 Effect of bubble flooding on shear behaviour of gassy Comwich mud: (a) the $\varepsilon_a - q$**
517 **relationship; (b) the effective stress path and (c) the evolution of excess pore water**
518 **pressure**

519

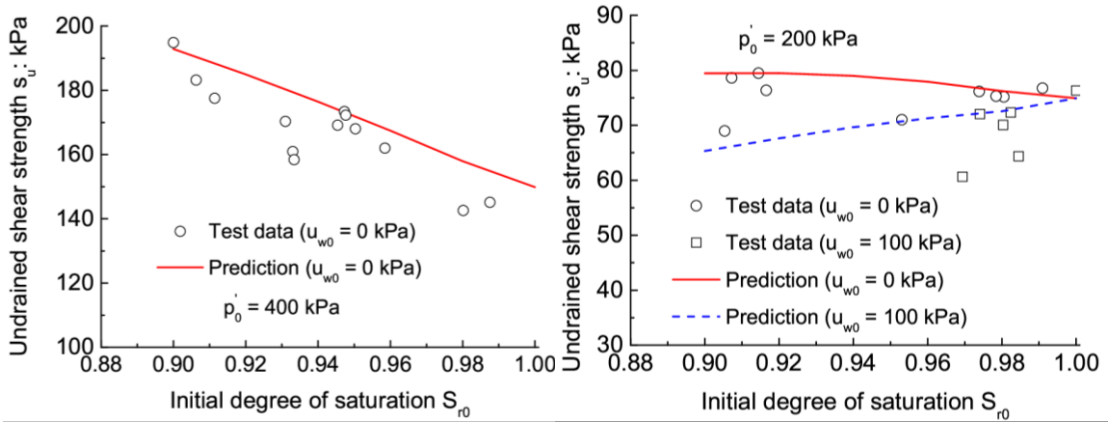

(a) (b)

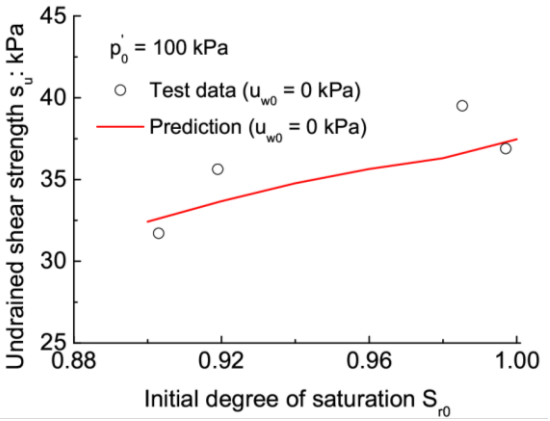

(c)

Fig. 4 Model prediction for the undrained shear strength of gassy Combwich mud: (a) $p_0' = 400$ kPa; (b) $p_0' = 200$ kPa and (c) $p_0' = 100$ kPa

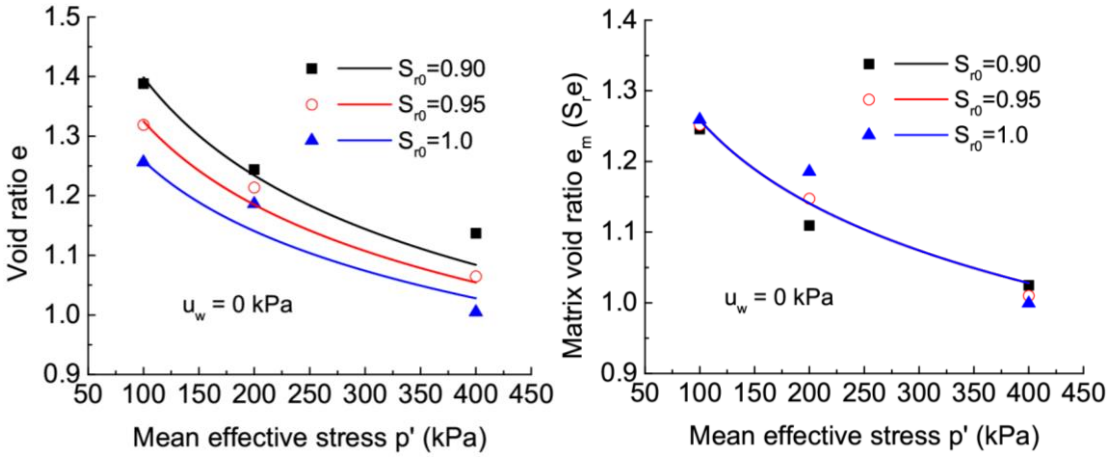

527

528 **(a)** **(b)**

529 **Fig. 5 Model prediction for isotropic consolidation of gassy Combwich mud: (a) the $e - p'$**
530 **relationship and (b) the $e_m - p'$ relationship**

531

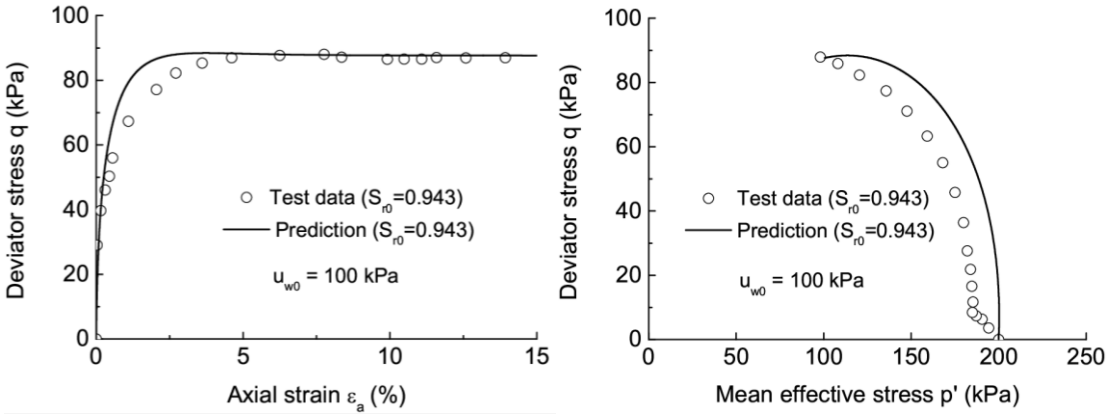

532

533 **(a)** **(b)**

534 **Fig. 6 Model prediction for the shear behaviour of gassy Kaolin with $p_0' = 200$ kPa, $u_{w0} =$**
535 **100 kPa and $s_{r0} = 0.943$: (a) the $\varepsilon_a - q$ relationship; (b) the effective stress path**

536

537

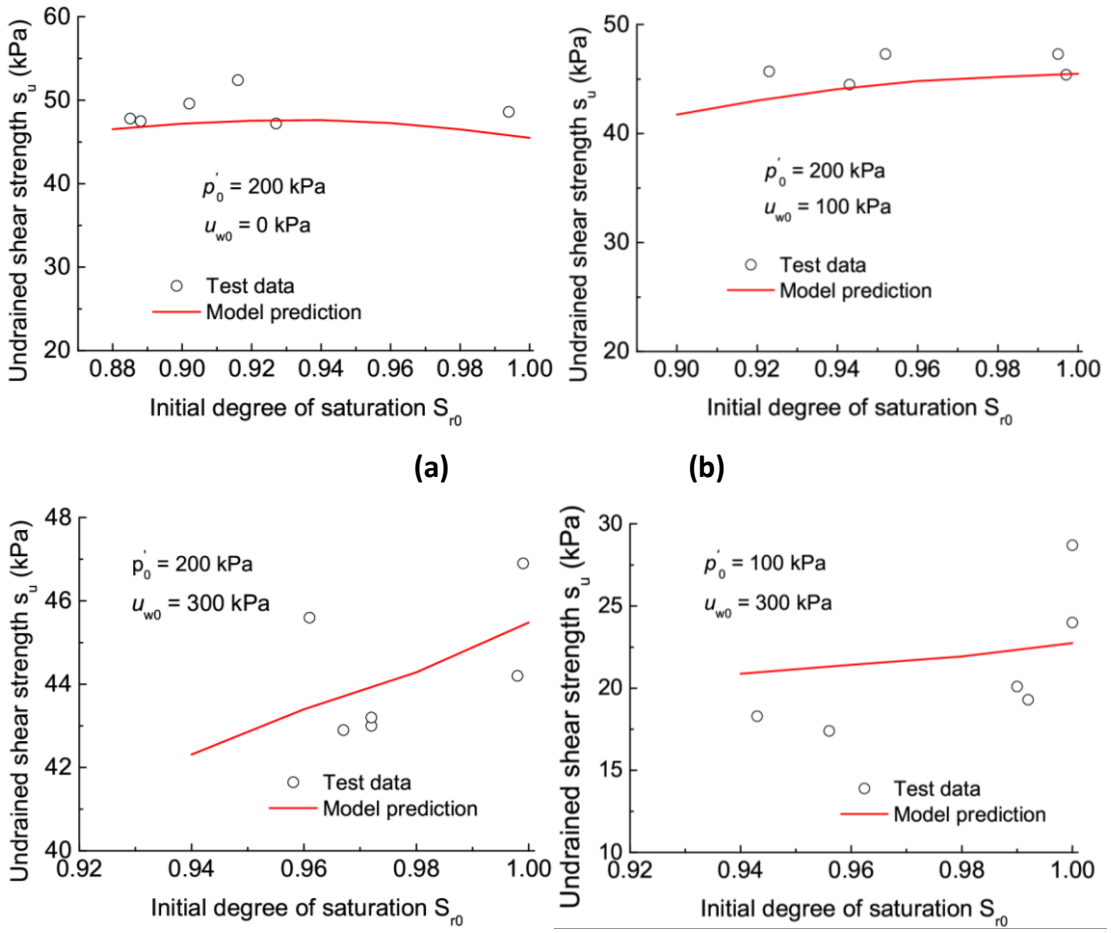

Fig. 7 Model prediction for the undrained shear strength of gassy Kaolin clay: (a) $p_0' = 200$ kPa and $u_{w0} = 0$ kPa; (b) $p_0' = 200$ kPa and $u_{w0} = 100$ kPa (c) $p_0' = 200$ kPa and $u_{w0} = 300$ kPa; (d) $p_0' = 100$ kPa and $u_{w0} = 300$ kPa

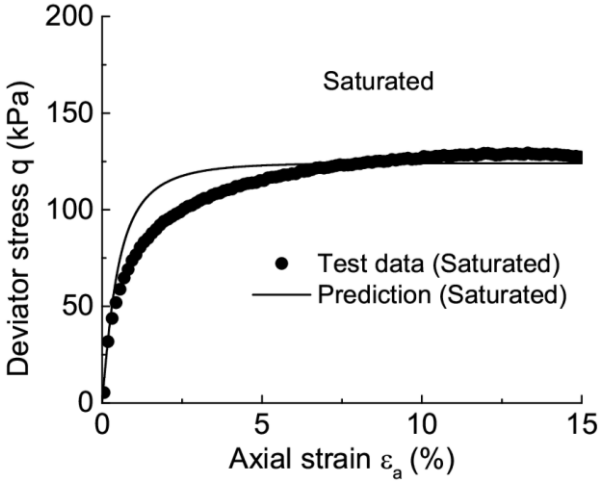

(a)

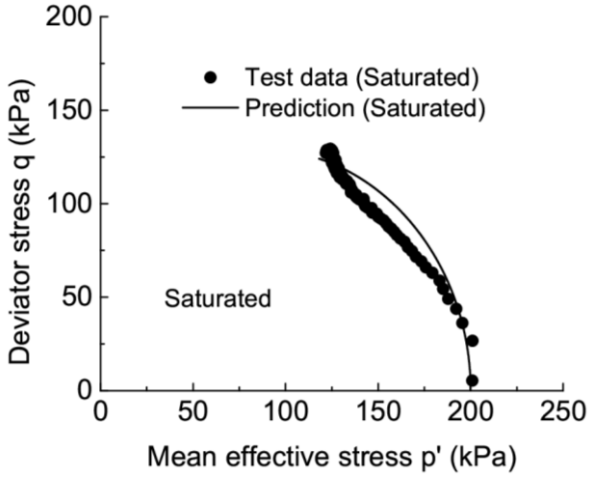

(b)

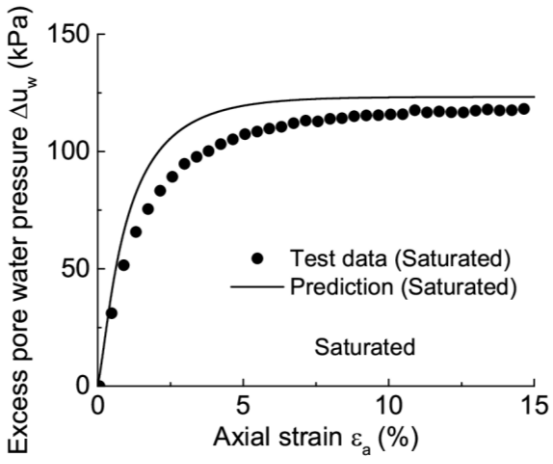

(c)

Fig. 8 Model prediction for the undrained shear behaviour of saturated Malaysian kaolin (a) the $\varepsilon_a - q$ relationship; (b) the effective stress path and (c) the evolution of excess pore water pressure

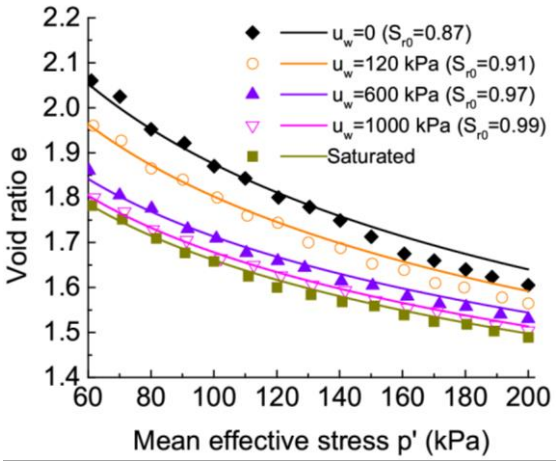

557

558 **Fig. 9 Model prediction for the isotropic consolidation of gassy Malaysian kaolin**

559

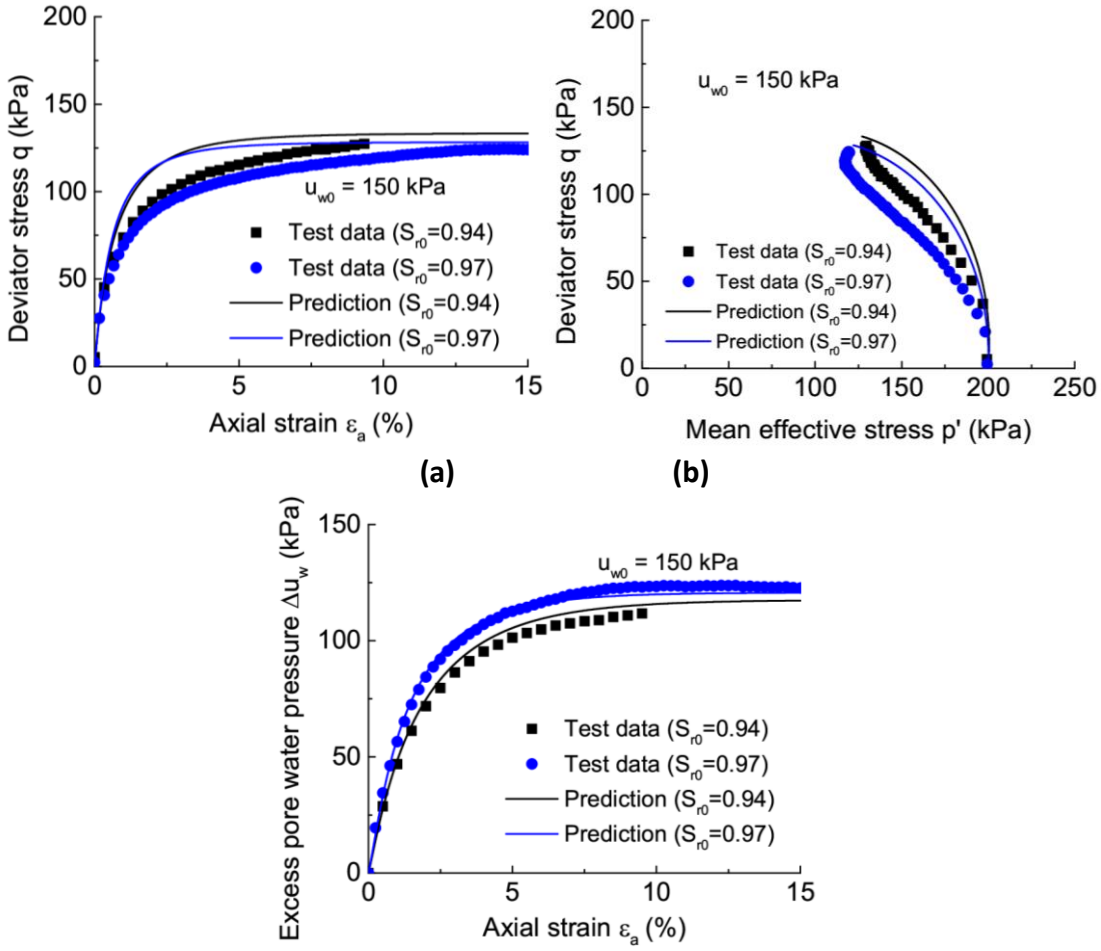

Fig. 10 Model prediction for the stress-strain relationship of gassy Malaysian kaolin with $p_0' = 200$ kPa and $u_{w0} = 150$ kPa: (a) the $\varepsilon_a - q$ relationship; (b) the effective stress path and (c) the evolution of excess pore water pressure

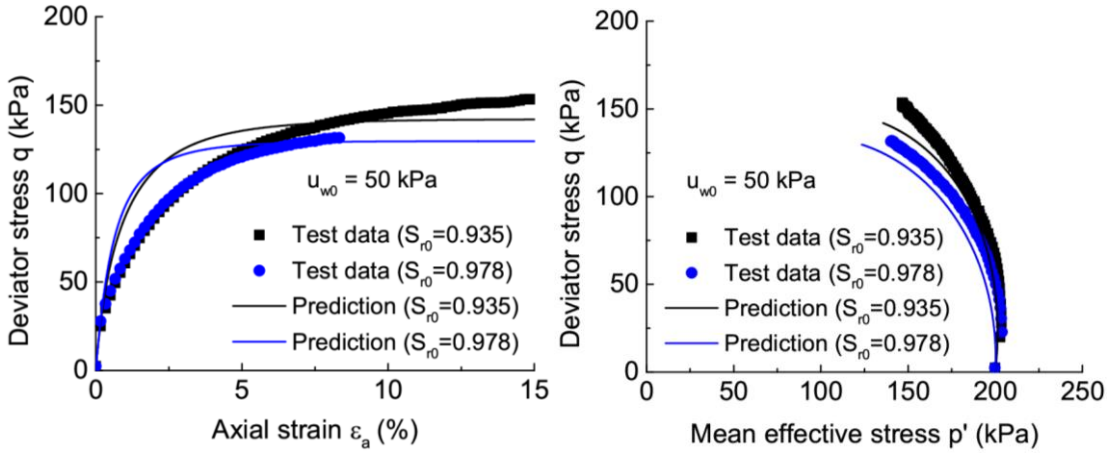

(a) (b)

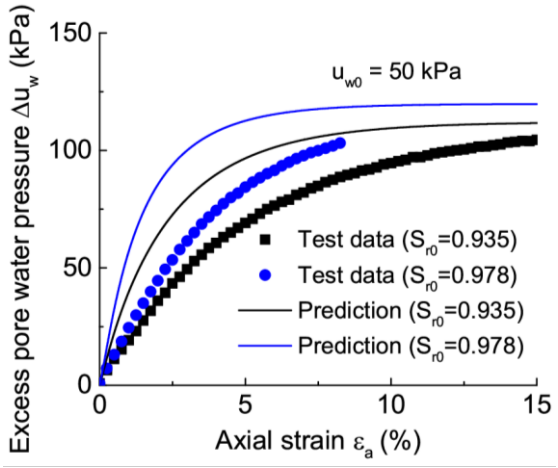

(c)

Fig. 11 Model prediction for the stress-strain relationship of gassy Malaysian kaolin with $p_0' = 200$ kPa and $u_{w0} = 50$ kPa: (a) the $\varepsilon_a - q$ relationship; (b) the effective stress path and (c) the evolution of excess pore water pressure

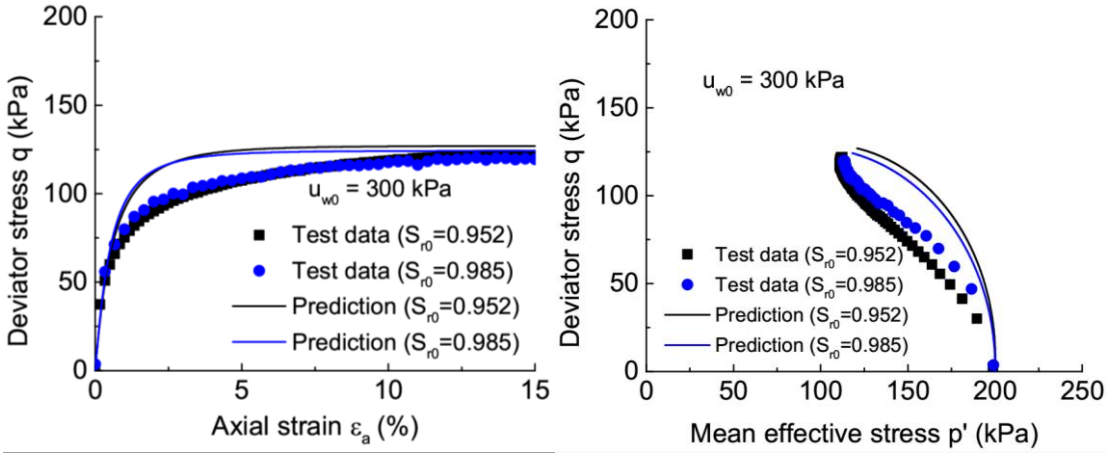

(a) (b)

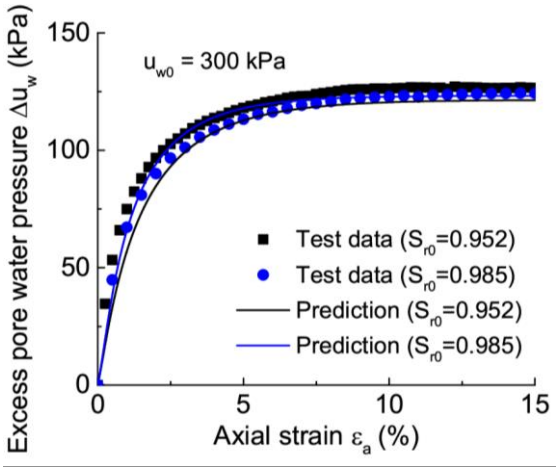

(c)

Fig. 12 Model prediction for the undrained shear behaviour of gassy Malaysian kaolin with $p_0' = 200$ kPa and $u_{w0} = 300$ kPa: (a) the $\varepsilon_a - q$ relationship; (b) the effective stress path and (c) the evolution of excess pore water pressure

Table 1 Model parameters

Soil	M	λ	κ	N	ν	a
Combwich mud (Wheeler, 1986)	1.33	0.174	0.0297	3.06	0.2	14
Kaolin clay (Sham, 1989)	0.87	0.23	0.014	3.35	0.2	15
Malaysian kaolin silt (Hong et al., 2020)	1.05	0.25	0.06	3.81	0.2	3